Hindawi
Shock and Vibration
Volume 2020, Article ID 9362434, 11 pages
https://doi.org/10.1155/2020/9362434

Research Article

Structural Modal Analysis and Optimization of SUV Door Based on Response Surface Method

Hao Chen,[1,2] Chihua Lu,[1,2] Zhien Liu,[1,2] Cunrui Shen,[1,2] Yi Sun,[1,2] and Menglei Sun[1,2]

[1]*Hubei Key Laboratory of Advanced Technology for Automotive Components, Wuhan University of Technology, Wuhan 430070, China*
[2]*Hubei Collaborative Innovation Center for Automotive Components Technology, Wuhan 430070, China*

Correspondence should be addressed to Zhien Liu; lzen@whut.edu.cn

Received 21 August 2019; Revised 30 November 2019; Accepted 31 December 2019; Published 20 January 2020

Academic Editor: Giuseppe Petrone

Sensitivity analysis and response surface methods were employed to optimize the structural modal of SUV doors. A finite element numerical simulation model was established and was calibrated by restraint modal tests. To screen out highly sensitive panels, a sensitivity analysis for the thickness of door panels was proposed based on the fifth-order modal frequency of the door. Data points were obtained by a faced central composite design with the design variables from the thickness of the highly sensitive panels, and a second-order explicit response surface function of the fifth-order modal frequency of the vehicle door was established. An optimization model was established according to the response surface method. The final results demonstrate that the modal-frequency matching of the door and body in white was optimized after changing the thicknesses, with a 5.74% material reduction.

1. Introduction

A modal analysis is an important method to study the performance of automotive noise, vibration, and harshness (NVH). Modal matching is based on the modal analysis of the reasonable distribution of structural modal frequencies. Modal frequency distribution is an important part of a vehicle body and has a great influence on its dynamic performance. When the modal frequency matching between the door and the body is unreasonable, the modal coupling between the structures is stronger to increase the body structural vibrations. Therefore, it is important to match the modal frequencies of the door and the body for the design of the door structure. For example, Shin et al. [1] suggested a design flow for topology, size, and shape optimization methods to improve the automotive door structure for better performance. Fang et al. [2] proposed a multiobjective reliability-based design optimization procedure to develop the design of the vehicle door. Sun et al. [3] employed a compromise programming approach and mean-frequency method to handle multiobjective optimization of an automotive door, which involves stiffness and natural-frequency criteria for multiple load cases. Lee and Kang [4] combined the kriging interpolation method with a simulated annealing algorithm for the design of a frontal door. Zhu et al. [5] integrated a finite element analysis, artificial neural network, and genetic algorithm for the optimal design of an inner door panel. Cui et al. [6] developed a multimaterial configuration for a lightweight design by combining a multiobjective genetic algorithm with an artificial neural network. The majority of door studies only analyses and optimizes the performance of a certain aspect of the door [7, 8]. There are few studies that comprehensively consider the structural modality, stiffness, and weight reduction of the door.

In the field of engineering design research, establishing high-fidelity models requires numerous resources. An approximate model of a response is established and used to analyse the response. The response surface method (RSM) combined with the finite element method can effectively calculate and optimize structural modal problems. An article by Box and Hunter [9] describes the rationale for RSM, which is to fit response surface functions related to inputs and outputs using a small number of strictly selected data sets in the design space. RSM has been applied in many research areas, such as experimental design and engineering structural analysis to

optimize modal or vibration problem [10–13]. Lee et al. [14] employed structural optimization to design the domains and thicknesses of the door for better stiffness. Although the RSM has been successfully applied to reduce the structural vibration [15, 16]; literatures about the optimization of panel thickness for the control of structural vibration are handful. For example, Lee and Kang [4] optimized the thicknesses of the parts to reduce the weight, and the RSM is not used.

In this study, according to the modal analysis results of a door, a sensitivity analysis of the thickness of each panel is conducted. The key panels affecting the modal performance of the door are selected as design variables to perform faced central composite design (FCCD). RSM is employed to establish the approximate model and optimize the door. The modal matching of the door and the body in white is optimized to improve the door modal performance while achieving a lightweight door.

2. Theory of the Response Surface Method

RSM is based on employing statistical and experimental techniques, when reasonably applied, to address more configurations of the input parameters to be tested and explore deeply the domain of the problem's solutions. The response surface function is a smooth, explicit, and analytic form obtained simply by carrying out limited experimental runs and regression analyses. The construction process of the response surface function is illustrated as follows.

2.1. Construction of Response Surface Function. The relationship between the system response of interest denoted by y and design factors denoted by vector $\mathbf{x} = (x_1, x_2, \ldots, x_n)$ is

$$y = f(x_1, x_2, \ldots, x_n) + \varepsilon, \tag{1}$$

where ε is the random experimental error term and its mean value is zero and $f(x_1, x_2, \ldots, x_n)$ is a function of $\mathbf{x}$ whose elements consist of powers and cross products of powers of $x_1, x_2, \ldots, x_n$ up to a certain degree. For many practical engineering applications, the order of polynomial $f(x_1, x_2, \ldots, x_n)$ is not more than three [15, 17–19]. In terms of the second-order response surface function, $f(x_1, x_2, \ldots, x_n)$ is expressed as

$$f(x, \alpha) = \alpha_0 + \sum_{i=1}^{n} \alpha_i x_i + \sum_{i=1}^{n} \alpha_{ii} x_i^2 + \sum_{i=1}^{n} \sum_{j<i} \alpha_{ij} x_i x_j. \tag{2}$$

To estimate the unknown parameter vector $\boldsymbol{\alpha} = (\alpha_0, \alpha_1, \ldots, \alpha_n, \alpha_{11}, \ldots, \alpha_{nn}, \alpha_{12}, \ldots, \alpha_{(n-1)n})$, a series of experiment runs are conducted, and the corresponding responses y are measured. At the kth experimental run, the design factor $\mathbf{x}$ is set to $x^k = (x_1^k, x_2^k, \ldots, x_n^k)$, and y^k denotes the corresponding response value. We then have

$$\begin{aligned} y^k = f\left(x_1^k, x_2^k, \ldots, x_n^k\right) + \varepsilon^k = \alpha_0 \\ + \sum_{i=1}^{n} \alpha_i x_i^k + \sum_{i=1}^{n} \alpha_{ii} \left(x_i^k\right)^2 + \sum_{i=1}^{n} \sum_{j<i}^{n} \alpha_{ij} x_i^k x_j^k + \varepsilon^k. \end{aligned} \tag{3}$$

Equation (3) can be rewritten in the matrix form as

$$\mathbf{y} = \mathbf{X}\boldsymbol{\alpha} + \boldsymbol{\varepsilon}, \tag{4}$$

$$\mathbf{X} = \begin{bmatrix} 1 & x_1^1 & \cdots & x_n^1 & \left(x_1^1\right)^2 & \cdots & \left(x_n^1\right)^2 & x_1^1 & x_2^1 & \cdots & x_{n-1}^1 & x_n^1 \\ \vdots & \vdots & & \vdots & \vdots & & \vdots & \vdots & \vdots & & \vdots & \vdots \\ 1 & x_1^k & \cdots & x_n^k & \left(x_1^k\right)^2 & \cdots & \left(x_n^k\right)^2 & x_1^k & x_2^k & \cdots & x_{n-1}^k & x_n^k \\ \vdots & \vdots & & \vdots & \vdots & & \vdots & \vdots & \vdots & & \vdots & \vdots \\ 1 & x_1^m & \cdots & x_n^m & \left(x_1^m\right)^2 & \cdots & \left(x_n^m\right)^2 & x_1^m & x_2^m & \cdots & x_{n-1}^m & x_n^m \end{bmatrix}, \tag{5}$$

in which $\mathbf{X}$ is a matrix of order $m \times p\,(p = (n+1)(n+2)/2)$, $\mathbf{y} = (y^1, y^2, \ldots, y^m)^T$, and $\boldsymbol{\varepsilon} = (\varepsilon^1, \varepsilon^2, \ldots, \varepsilon^m)^T$, respectively. Equations (4) and (5) indicate that the number of unknown coefficients $\boldsymbol{\alpha}$ is $(n+1)(n+2)/2$. Thus, an equal or greater number of experiments (i.e., $m \geq p$) is required to estimate these parameters. The coefficient vector $\boldsymbol{\alpha}$ is estimated by the ordinary least-squares estimator [20] given by

$$\boldsymbol{\alpha} = \left(\mathbf{X}^{\mathrm{T}}\mathbf{X}\right)^{-1}\mathbf{X}^{\mathrm{T}}\mathbf{y}. \tag{6}$$

2.2. Design of Experiment

2.2.1. Faced Central Composite Design. The design of a series of experimental runs allows highly relevant information data that reflect the design goals with minimal resources and time to be obtained. For the design of the experiment, it is important to select a set of data points within the design domain. A set of poor data points affects the accuracy of the established RSM. Compared with the central composite design [15, 21], the axis points of the FCCD are set to levels 1 or −1, which limits the design variables to the design domain. Compared with the full-factorial design, the FCCD requires fewer data points without significantly affecting the accuracy. For example, as to a problem having the four-factor-three-levels, the number of experimental runs of the full-factorial design is $3^n = 81$, whereas it is $2^n + 2n + 1 = 25$ for FCCD. The number of required simulations and the computational costs are reduced drastically by adopting FCCD.

2.2.2. Model Validation. The RSM can replace the actual system equivalently if the actual responses are fitted well by

the established RSM. The adjusted coefficient of multiple determination is usually employed to verify the RSM in engineering, and the mathematical formulations are given by [22]

$$S_z = \sum_{k=1}^{n} \left(y^k - \overline{y}\right)^2, \tag{7}$$

$$f_z = n - 1, \tag{8}$$

$$S_c = \sum_{k=1}^{n} \left(y^k - \widehat{y}^k\right)^2, \tag{9}$$

$$f_c = n - \frac{(k+1)(k+2)}{2}, \tag{10}$$

where y^k and $\widehat{y}^k$ are the modal frequency responses calculated using the finite element method and response surface function, respectively, in the kth experimental run and $\overline{y}$ is the geometric mean of y. According to equations (7)–(10), the formulation of adjusted coefficient of multiple determination is

$$R^2_{\text{adj}} = 1 - \frac{S_c}{S_z}\frac{f_z}{f_c}. \tag{11}$$

For a good fit, R^2_{adj} should be closer to 1.

2.2.3. Vehicle Door Optimization Procedure. The establishment of the vehicle door finite element model is conducted in HYPERWORKS software. The flowchart of the iteration procedure is shown in Figure 1. A second-order explicit response surface function of the fifth-order modal frequency of the vehicle door is established based on the sensitivity analysis and FCCD. The design variables, constraint functions, and objective functions are set in the Isight software, and the sequential quadratic programming method is selected to continuously seek the optimal solution. The design is a single-objective multiconstraint problem, and the optimal solution of the design variables is obtained.

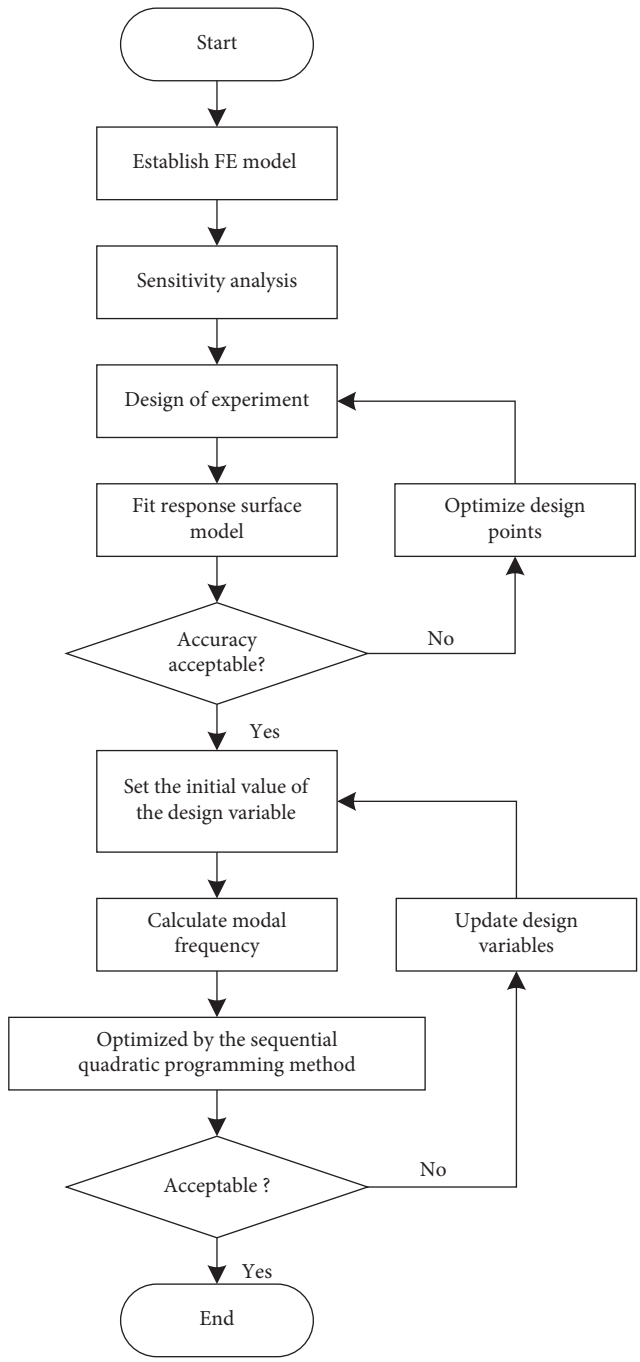

Figure 1: Flowchart of the optimization procedure.

3. Numerical Model and Validation of the Vehicle Door

The preprocessing of the finite element model is conducted in HYPERWORKS software, and the model is computed using MSC.NASTRAN software. The vehicle door comprises thin-walled parts (including inner and outer panels, support panels, interior panels, and glass) meshed using the shell element of four modes or three nodes. To avoid the model stiffness becoming too large to be accurate, the number of three-node shell elements is restricted to not more than 3% in the finite element model. The material of the vehicle door structure is ordinary steel (Young modulus $E = 2.1 \times 10^5$ MPa, mass density $\rho = 7.8 \times 10^3$ kg/m^3, Poisson's ratio $\mu = 0.3$, and no damping) and glass (Young modulus $E = 6.9 \times 10^4$ MPa, mass density $\rho = 2.5 \times 10^3$ kg/m^3, Poisson's ratio $\mu = 0.3$, and no damping), respectively. Spot welding is used to connect the door parts, which is simulated with the element ACM2 (i.e., six-sided solid element and interpolation constraint element). The bonding material is adhesive (Young modulus $E = 50$ MPa, mass density $\rho = 1.2 \times 10^3$ kg/m^3, Poisson's ratio $\mu = 0.49$, and damping coefficient 0.1). There are 34186 elements and 981 (2.87%) three-node shell elements in the vehicle door. The constrained mode of the vehicle door model is computed using the modal superposition method. In the finite element model, rotation around the Z-axis at the hinge of the door is released, and translation in the Y-direction of the door-lock installation is constrained. The coordinate system of the finite element model is consistent

with the vehicle coordinate system of the vehicle. To reduce the truncation error of the modal superposition method, the end frequency of the modal method is at least twice that of the upper limit of the calculated frequency.

A door constraint modal test was carried out to verify the accuracy of the established numerical simulation model. For the structure of the door, 50 points of vibration data are acquired by a single-point excitation single-point measurement method. The results of the numerical simulation and modal test are listed in Table 1. The simulation mode is demonstrated to be consistent with the experimental mode shape, and the relative error is within the acceptable range. This indicates that the numerical simulation model can simulate the dynamic performance of the actual door structure well, and the numerical simulation model has higher precision.

The fifth-order mode shape of the door is shown in Figure 2. The mode shape is mainly the local vibration of the inner panel of the door. The vibration is in the left inner plate and the right inner plate of the door. The door is fixed on the body in white through the rotating hinge and the door closing. The eighth-order frequency of the body in white is 54.56 Hz (Figure 3), which is close to the fifth-order modal frequency of the door and easily generates structural resonance. The modal frequency distributions of the door and the body in white have an interval of more than 2 Hz, which realizes modal separation. The fifth-order mode of the door and the body-in-white mode are not well matched and need to be improved.

4. Response Surface Model of Modal Frequency

4.1. Sensitivity Analysis of Modal Frequency with respect to Panel Thickness. The door structure is connected by numerous thin-walled structures, and the modal distribution of the door structure can be improved by optimizing the thickness-matching of the plates. Before optimizing the thickness of the door panel, the sensitivity of the door modal frequency to the thickness of the door panel is first studied. Sensitivity is used to calculate the sensitivity of structural response to each design variable, to reflect the influence of structural design variables on structural performance, and to find the most sensitive parts. This method is more targeted in obtaining design variables and greatly improves the optimization efficiency.

The sensitivity of the door modal frequency to the thickness of the door panel is

$$S\left(\frac{f}{X}\right) = \frac{\partial f(X)}{\partial X}, \tag{12}$$

where $f(X) = f(x_1, x_2, \ldots, x_n)$ is the structural modal frequency of the door, which is a function of the plate thickness variable $X = (x_1, x_2, \ldots, x_n)$, and x_i is the thickness of the ith panel. Then, the sensitivity of the jth-order modal frequency with respect to the thickness of the ith panel is

$$S_{ji} = \frac{\partial f_j(X)}{\partial x_i} = \frac{\partial f_j(x_1, x_2, \ldots, x_i, \ldots, x_n)}{\partial x_i}. \tag{13}$$

It is customary to use differential equations to approximate the partial differential in engineering, and then the central differential expression of the sensitivity of the jth-order modal frequency with respect to the thickness of the ith panel is

$$S_{ji} = \frac{\partial f_j(X)}{\partial x_i} \approx \frac{1}{2\Delta x_i}\Big(f_j(x_1, x_2, \ldots, x_i + \Delta x_i, \ldots, x_n) - f_j(x_1, x_2, \ldots, x_i - \Delta x_i, \ldots, x_n)\Big). \tag{14}$$

The sensitivity of the fifth-order modal frequency of the door to the thickness of the panels is studied based on this theoretical methodology. The primary selection variables are the right inner panel thickness t_1, left inner panel thickness t_2, inner reinforcing panel thickness t_3, window-frame vertical-reinforcing panel thickness t_4, outer panel thickness t_5, window-frame horizontal-reinforcing panel thickness t_6, and side-impact beam thickness t_7. To reduce the influence of the difference in each panel mass on the sensitivity, the sensitivity solved by equation (14) is divided by the original mass of each panel (sensitivity value of the frequency per unit mass with respect to the panel thickness), $\Delta x_i = 0.05x_i$, in equation (14). By using equation (14) and the door finite element model, the sensitivity results of the calculated fifth-order modal frequencies with respect to the thickness of the panel are summarized in Table 2. It can be seen that the sensitivity results of the fifth-order modal frequency of the door on the right inner panel, left inner panel, inner reinforcing panel, window-frame vertical-reinforcing panel, and the outer panel are large with respect to the thickness of the panel—29.71, 3.79, −0.33, 0.50, and −1.43 Hz/mm, respectively.

Per unit mass, the sensitivity values of the modal frequencies of the right inner panel, left inner panel, inner reinforcing panel, window-frame vertical-reinforcing panel, and outer panel are relatively large with respect to the thickness of the panel—8.25, 1.40, −1.04, and 1.09 Hz/mm·kg, respectively. This indicates that changing the thickness of these plates per unit mass changes the value of the fifth-order modal frequency significantly. Among them, the sensitivities of t_1, t_2, and t_4 are positive numbers; it is indicated that, within a certain range, the fifth-order frequency f_5 of the door gradually increases with increasing panel thickness, and the increasing speed is more obvious. The sensitivity of t_3 is negative; it is indicated that, within a certain range, the fifth-order frequency f_5 of the door gradually increases with decreasing plate thickness, and the increasing speed is more obvious. t_1, t_2, t_3, and t_4 are selected as the design variables (respectively, labelled as x_1, x_2, x_3, and x_4). By changing the thickness of the panel, the fifth-order modal frequency of the door can be effectively improved under the premise that the door mass does not increase significantly. Optimize the matching between the door mode and the body in white mode. The key panels are selected from many structural panels through a sensitivity study of the fifth-order modal frequency f_5 on the thickness of the panel; this better targets the variables to be optimized and reduces the scale of the model to be optimized.

Table 1: Comparison of modal results of simulation and experiment.

Frequency calculated f_s (Hz)	Frequency tested f_s (Hz)	Relative error e (%)	Description of modal
42.72	40.92	4.4	Bending mode of the beam
51.52	49.67	3.7	1st bending mode
55.34	55.27	0.1	1st torsional mode
71.04	71.49	−0.6	Bending and torsional model

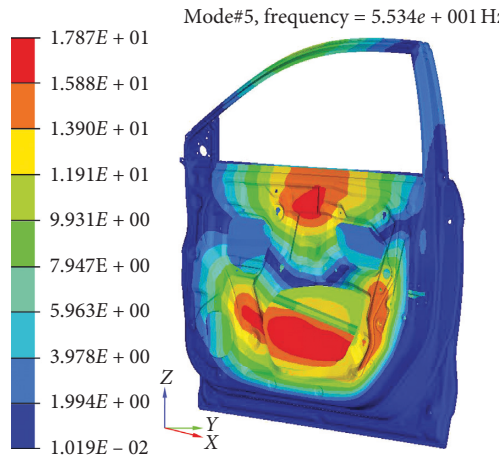

Figure 2: Fifth-order structure mode of the door.

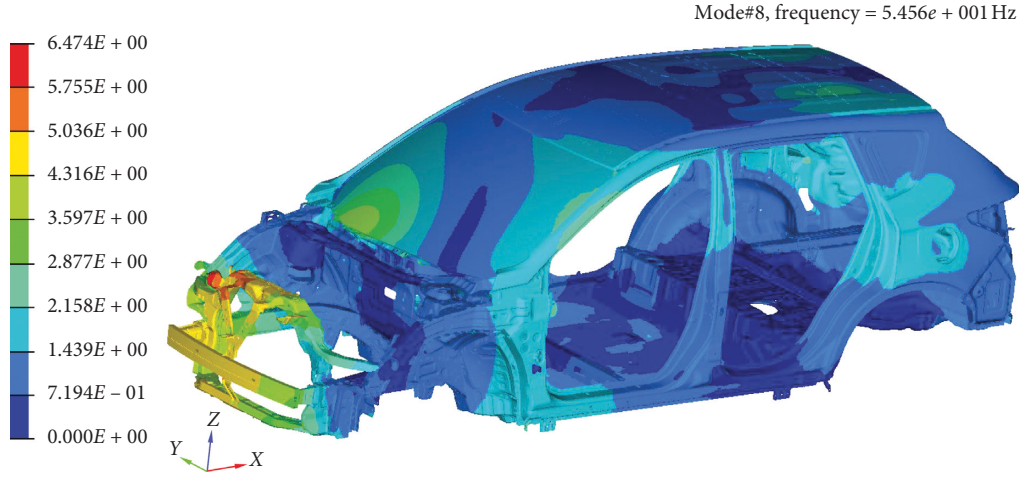

Figure 3: Eighth-order structure mode of the body in white.

Table 2: Sensitivity of the fifth-order modal frequencies to panel thickness.

Panel thickness (mm)	Mass (kg)	S_{5i} (Hz/mm)	S_{5i}/m_i (Hz/mm·kg)
t_1	3.60	29.71	8.25
t_2	2.71	3.79	1.40
t_3	0.32	−0.33	−1.04
t_4	0.46	0.50	1.09
t_5	4.84	−1.43	−0.30
t_6	0.43	−0.25	−0.58
t_7	1.48	0.36	0.25

4.2. Design Variables. Considering the processing requirements of each panel, the thickness ranges of the panels are designed as summarized in Table 3.

4.3. Design of Experiment for Modal Frequency. To establish the response surface functions of the modal frequency, FCCD is developed to generate an efficient set of data points and the

Table 3: Range of design variables of the corresponding panel.

Design variable	Lower bound (mm)	Original thickness (mm)	Upper bound (mm)
x_1	0.5	0.7	0.9
x_2	1.2	1.4	1.6
x_3	0.5	0.6	0.8
x_4	0.6	0.8	1.0

corresponding modal frequency responses y by using the finite element method. Each design factor is set at three levels. Thus, a four-factor-three-level FCCD is developed (see Table 4). There are 25 experimental runs, which are higher than the number of unknown coefficients to be computed. The 2nd–5th columns of Table 4 are the values of the design factors at each experimental run, and the 6th and7th columns are the corresponding modal frequency responses.

4.4. Second-Order Response Surface Model. According to equations (2), (4), and (6) and the design of experiments provided in Table 4, the second-order polynomial $f(x, \alpha)$ of the 8th modal frequency is given as follows:

$$\begin{aligned} f(x) &= f(x_1, x_2, x_3, x_4) \\ &= 22.7832 + 40.6830x_1 + 7.8626x_2 \\ &\quad + 2.8563x_3 + 4.6872x_4 - 22.6137x_1^2 \\ &\quad - 3.4887x_2^2 - 2.4033x_3^2 - 1.1137x_4^2 + 8.3750x_1x_2 \\ &\quad - 0.5671x_1x_3 - 3.5312x_1x_4 - 0.0061x_2x_3 \\ &\quad + 0.8438x_2x_4 + 0.4299x_3x_4. \end{aligned} \tag{15}$$

The modal frequency responses are calculated according to equation (15), and the results are presented in Table 4. The 8th column of Table 4 shows the results of the relative errors between the RSM and finite element method. The expression of relative error is presented in equation (16), where $y_{\mathrm{FEM}}(i)$ and $y_{\mathrm{RSM}}(i)$ are the modal frequency response of the ith experimental run calculated by the finite element method and RSM, respectively. It should be noted from Table 4 that the relative errors are small for all experimental runs, and thus, the experimental points are fitted well by the modelled second-order response surface function $f(x)$.

$$\varepsilon_{\mathrm{RE}}(i) = \frac{y_{\mathrm{RSM}}(i) - y_{\mathrm{FEM}}(i)}{y_{\mathrm{FEM}}(i)} \times 100\%. \tag{16}$$

4.5. Verification of the Response Surface Model. The accuracy of the response surface function needs to be evaluated before employing the response surface function for door structural modal analysis and optimization. The adjusted coefficient of multiple determination is employed. The R^2_{adj} value of the response surface function is obtained as 0.996 using equation (11); R^2_{adj} is close to one. This means that the effectiveness of the response surface function is good.

To illustrate the accuracy of the response surface function further, several trial data points are calculated, and the results are presented in Table 4. The relative errors $\varepsilon_{\mathrm{RE}}$ of all trial experimental runs are small, and thus, the data points in the design region can be fitted effectively by the response surface function $f(x)$. The 6th and 7th columns of Table 4 are the calculation times of each experimental run on a 2.60-GHz PC. The calculation time for a single run by using the RSM is substantially lower than that of the finite element method. This is because numerous coupled nonlinear governing differential equations need to be triangulated and calculated by using the finite element method, whereas the calculation equation is a simple explicit form in the response surface method.

The calculated results of R^2_{adj} show that the response surface function $f(x)$ is highly accurate. The model reflects the relationship between modal frequency response and design variables effectively. Therefore, it is feasible to employ the RSM instead of the finite element model to study the structural modal analysis and optimize the door panels.

Table 4: FCCD of the fifth-order modal frequencies to design variables.

No.	Thickness of vehicle door panel				Response y (Hz)		$\varepsilon_{\mathrm{RE}}$ (%)
	x_1 (mm)	x_2 (mm)	x_3 (mm)	x_4 (mm)	FEM	RSM	
1	0.5	1.2	0.5	0.6	49.54	49.68	0.28
2	0.5	1.2	0.5	1.0	50.73	50.62	−0.21
3	0.5	1.2	0.8	0.6	49.46	49.59	0.26
4	0.5	1.2	0.8	1.0	50.68	50.59	−0.19
5	0.5	1.6	0.5	0.6	50.86	50.79	−0.13
6	0.5	1.6	0.5	1.0	51.86	51.87	0.03
7	0.5	1.6	0.8	0.6	50.78	50.70	−0.16
8	0.5	1.6	0.8	1.0	51.81	51.83	0.05
9	0.9	1.2	0.5	0.6	56.33	56.35	0.03
10	0.9	1.2	0.5	1.0	56.65	56.73	0.14
11	0.9	1.2	0.8	0.6	56.24	56.19	−0.09
12	0.9	1.2	0.8	1.0	56.55	56.62	0.13
13	0.9	1.6	0.5	0.6	58.69	58.80	0.19
14	0.9	1.6	0.5	1.0	59.48	59.32	−0.27
15	0.9	1.6	0.8	0.6	58.55	58.64	0.16
16	0.9	1.6	0.8	1.0	59.31	59.21	−0.17
17	0.7	1.4	0.6	0.8	55.34	55.37	0.06
18	0.5	1.4	0.6	0.8	50.91	50.95	0.08
19	0.9	1.4	0.6	0.8	58.04	57.99	−0.09
20	0.7	1.2	0.6	0.8	54.49	54.31	−0.33
21	0.7	1.6	0.6	0.8	55.99	56.16	0.30
22	0.7	1.4	0.5	0.8	55.38	55.36	−0.04
23	0.7	1.4	0.8	0.8	55.25	55.26	0.02
24	0.7	1.4	0.6	0.6	55.24	54.95	−0.52
25	0.7	1.4	0.6	1.0	55.43	55.70	0.49

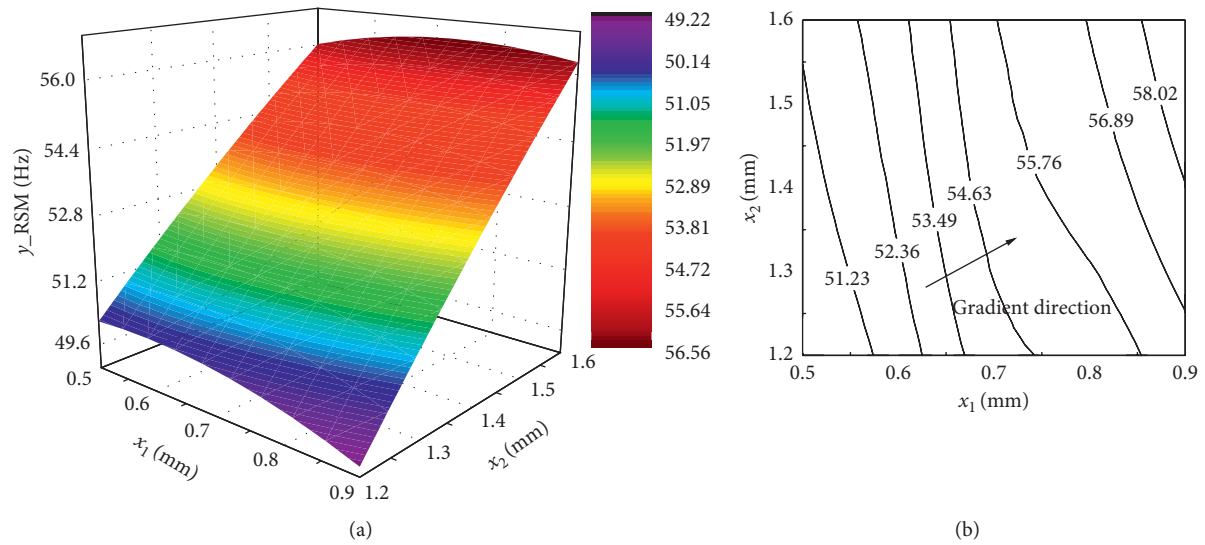

FIGURE 4: Modal frequency responses with respect to design factors x_1 and x_2. (a) Colour map surface of modal frequency. (b) Contour lines of modal frequency.

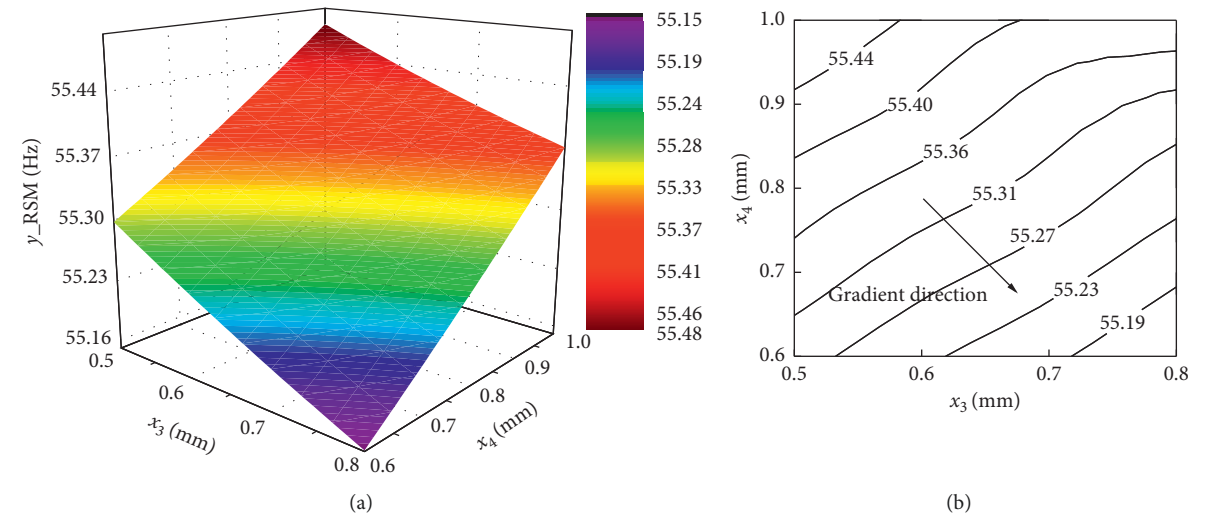

FIGURE 5: Modal frequency responses with respect to design factors x_3 and x_4. (a) Colour map surface of modal frequency. (b) Contour lines of modal frequency.

4.6. Structural Modal Analysis by Using the Response Surface Model. The response surface function is applied to study the relationship between the fifth-order modal frequency of the door and the design variables. The results are shown in Figures 4 and 5. It can be seen from Figure 4 that the fifth-order modal frequency of the door changes significantly with respect to x_1 and x_2, and the maximum and minimum values are 58.92 Hz ($x_1 = 0.9$ mm, $x_2 = 1.6$ mm) and 50.08 Hz ($x_1 = 0.5$ mm, $x_2 = 1.2$ mm), respectively; in Figure 4(b), the gradient direction of the contour line gives the direction of convergence of the variable when optimizing the modal frequency of the door from the side. It can be seen from Figure 5 that the fifth-order modal frequency of the door is insensitive to changes in x_3 and x_4; the frequency variation range is 55.15–55.45 Hz; and the door frequency and the body-in-white frequency cannot be isolated with optimization of only variables x_3 and x_4. Comparison of Figures 4 and 5 shows that the changes in x_1 and x_2 are sensitive to the fifth-order modal frequency of the door, and this conclusion is in agreement with the sensitivity analysis results in Table 2.

5. Vehicle Door Modal Frequency Optimization

Owing to the similarity of the fifth-order modal frequency of the door and the eighth-order modal frequency of the body in white, the door can be mounted on the body in white to easily cause structural resonance. Therefore, the door structure needs to be optimized to change the modal frequency distribution so that the fifth-order modal frequency of the door is staggered from the body-in-white modal frequency, and the frequencies of the other modes

Table 5: Values of objective function and design variables with respect to iteration process.

Iteration number	y_{obj} (Hz)	Design variable (mm)			
		x_1	x_2	x_3	x_4
0	55.369	0.7	1.4	0.6	0.8
1	55.382	0.7007	1.4	0.6	0.8
2	55.376	0.7	1.4014	0.6	0.8
3	55.369	0.7	1.4	0.6006	0.8
4	55.371	0.7	1.4	0.6	0.8008
5	49.666	0.5	1.2	0.69044	0.6
6	49.679	0.5005	1.2	0.69044	0.6
7	49.671	0.5	1.2012	0.69044	0.6
8	49.665	0.5	1.2	0.69113	0.6
9	49.667	0.5	1.2	0.69044	0.6006
10	49.583	0.5	1.2	0.8	0.6
11	49.596	0.5005	1.2	0.8	0.6
12	49.588	0.5	1.2012	0.8	0.6
13	49.584	0.5	1.2	0.7992	0.6
14	49.585	0.5	1.2	0.8	0.6006
15	49.583	0.5	1.2	0.8	0.6

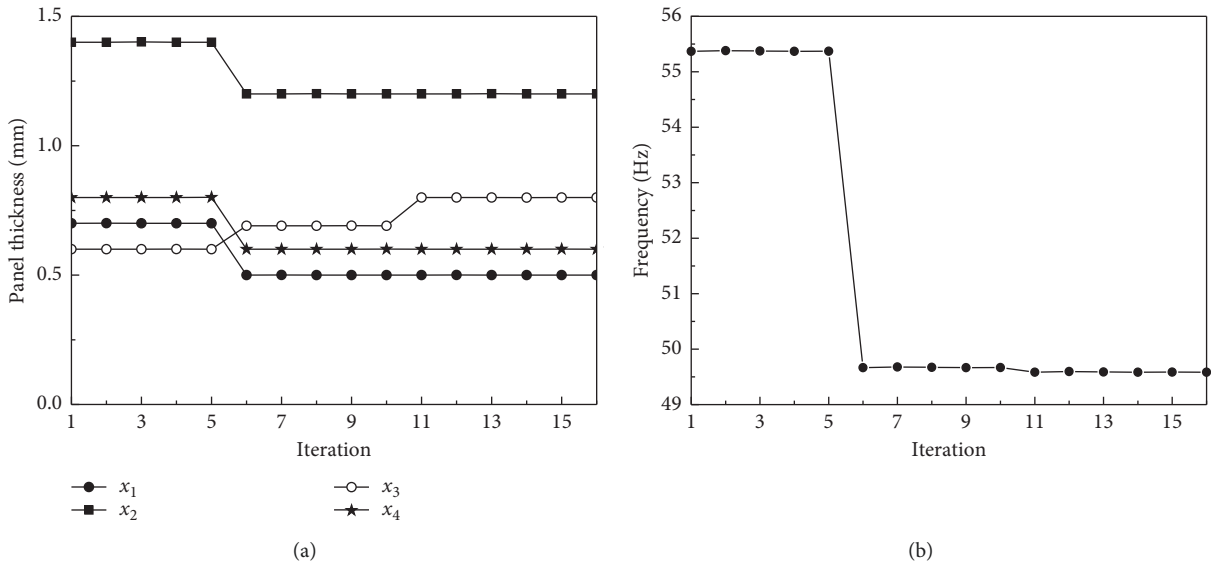

Figure 6: Values of objective function and design variables with respect to iteration process. (a) Values of design variables. (b) Values of objective function.

Table 6: Results of computational times and relative errors at experimental runs.

No.	Thickness of door panel (mm)				Calculation time (s)		Response (Hz)		ε_{RE} (%)
	x_1	x_2	x_3	x_4	FEM	RSM	FEM	RSM	
1	0.5	1.2	0.5	0.6	25.33	0.0231	49.54	49.68	0.28
2	0.5	1.6	0.5	1.0	24.78	0.0227	51.86	51.87	0.03
3	0.7	1.4	0.6	0.8	25.12	0.0219	55.34	55.37	0.06
4	0.9	1.4	0.6	0.8	25.06	0.0223	58.04	57.99	0.09

of the door are spaced from the body-in-white modal frequency. Moreover, the global Y-direction stiffness of the door is not reduced significantly so as to meet the side-impact requirements of the door. The fifth-order modal frequency RSM of the door can replace the finite element model with high precision to study the numerical relationship between the modal frequency and the thickness of the plate. Thus, a fifth-order modal frequency response surface function component optimization model of the door is applied. Considering x_1, x_2, x_3, and x_4 as design variables, the upper and lower limits of the constraint variables are shown in Table 3. The constraint

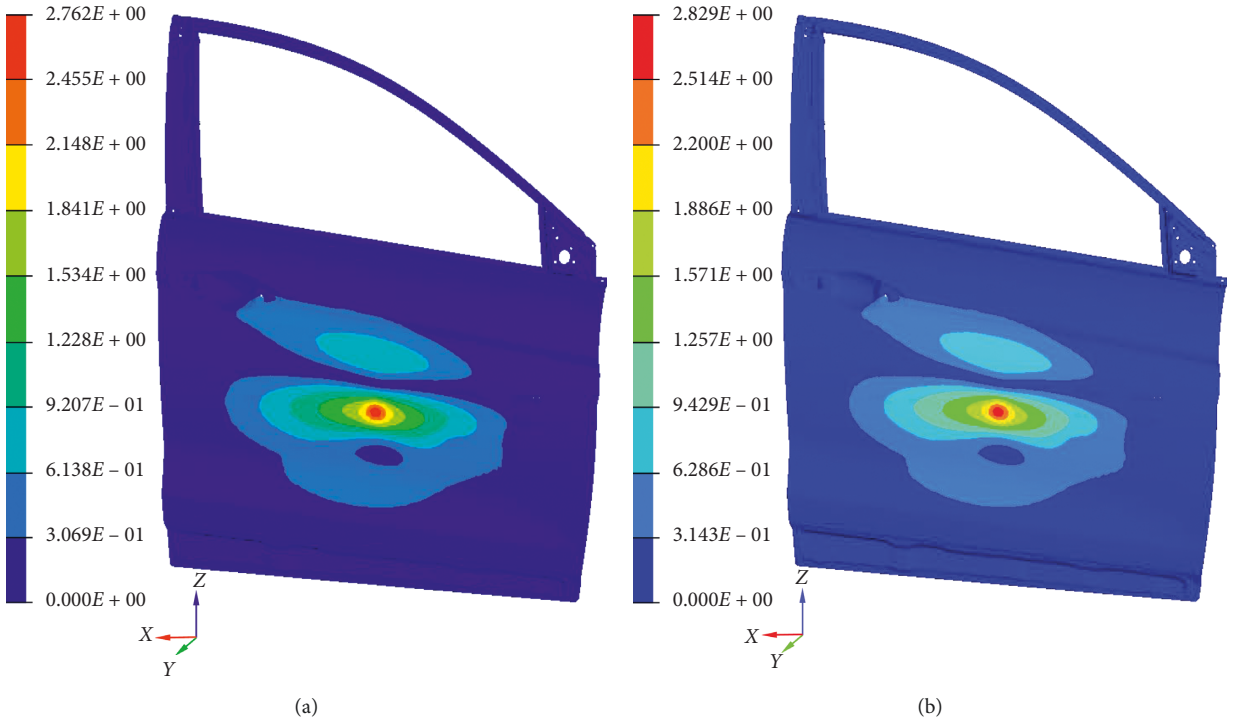

Figure 7: Displacement distribution before and after optimization under concentrated load. (a) Before optimization. (b) After optimization.

condition is that the door weight must be less than that of the original. The optimization goal is that the fifth-order modal frequency of the door differs from the eighth-order modal frequency of the body in white. The optimization model can be expressed as

$$\begin{cases} \max & \left| f(x_1, x_2, x_3, x_4) - f_{\text{BIW}} \right|, \\ \text{s.t.} & 0.5 \le x_1 \le 0.9 \\ & 1.2 \le x_2 \le 1.6 \\ & 0.5 \le x_3 \le 0.8 \\ & 0.6 \le x_4 \le 1.0 \\ & s_1 x_1 + s_2 x_2 + s_3 x_3 + s_4 x_4 \le s_1 x_{1\text{ori}} \\ & + s_2 x_{2\text{ori}} + s_3 x_{3\text{ori}} + s_4 x_{4\text{ori}}, \end{cases} \tag{17}$$

where f_{BIW} is the eighth-order frequency of the body in white; $s_1 = 0.654\,\text{m}^2$, $s_2 = 0.247\,\text{m}^2$, $s_3 = 0.068\,\text{m}^2$, and $s_4 = 0.073\,\text{m}^2$ are the areas of the right inner panel, left inner panel, inner reinforcing panel, and window-frame vertical-reinforcing panel, respectively; $x_{1\text{ori}} = 0.7\,\text{mm}$; $x_{2\text{ori}} = 1.4\,\text{mm}$; $x_{3\text{ori}} = 0.6\,\text{mm}$; and $x_{4\text{ori}} = 0.8\,\text{mm}$.

The optimization process is calculated by employing the sequential quadratic programming method in the Isight software optimization component. The optimal solution is obtained after 15 iterations. The values of the design variables and objective function at each iteration are provided in Table 5 and Figure 6. Evidently, as the number of iterations increases, x_1 reduces from 0.7 to 0.5 mm, x_2 reduces from 1.4 to 1.2 mm, x_3 increases from 0.6 to 0.8 mm, and x_4 reduces from 0.8 to 0.6 mm. The objective function reduces from 55.37 to 49.58 Hz. As shown in Table 6, the calculation time of the modal frequency optimization is 0.023 s, which is significantly less than that of the value for a single run of the finite element model. By using the optimization model (see equation (17)), the calculation time is low because the optimization model is a simple explicit function with a low number of iterations. In contrast, the computational time to optimize the same modal problem using the FE method is long because a large number of differential equations need to be triangulated and computed. The optimum solution of the design variables and objective function are summarized in Table 6. The thickness of t_1, t_2, t_3, and t_4 is 0.5, 1.2, 0.5, and 0.6 mm, respectively. The final values are 0.5, 1.2, 0.5, and 0.6 mm, respectively. The fifth-order modal frequency of the door is 40.50 Hz after optimization.

To verify the side-impact performance of the door after optimization, a force of 100 N is loaded in the centre of the outer panel of the door, in the Y-direction of the vehicle coordinate system, to calculate the deformation of the front and rear doors. The result is shown in Figure 7. The stiffness of the initial model at the loading point is 36.2 N/mm. After optimization, the stiffness of the model at the loading point is 35.3 N/mm; the stiffness is reduced by 2.5%. The Y-direction stiffness of the optimized door at the weak point is not significantly reduced and meets the requirements of side impact of the door. After the thickness of the panel is optimized by the RSM, the total door mass is 26.12 kg, which is 5.74% less than the original total door mass of 27.71 kg. The optimization of modal-frequency matching not only improves the dynamic performance of the structure but also reduces material and realizes a lightweight structure. At the same time, the side-impact performance of the door is not significantly reduced.

6. Conclusion

This paper proposed a sensitivity analysis method and response surface method to optimize the structural modal of an SUV door. A sensitivity analysis with respect to the thickness of the door panels was employed to screen out highly sensitive panels and identify the significant design variables. The FCCD was employed to obtain the data points. Then, the second-order response surface function was established, and an optimization model for the modal problem was proposed. From the results obtained, we can draw the following specific conclusions:

(1) The highly sensitive panel of the door was obtained by using the approximate sensitivity calculation of the central difference, and the corresponding panel thicknesses were selected as the design variables to more closely target the optimization of the door modal frequency.

(2) The response surface function of the fifth-order modal frequency of the door was established by obtaining a set of data points using the FCCD. This response surface function has a high fitting accuracy and can be used as a good substitute for the finite element model in the whole design domain, which significantly improves the calculation efficiency and saves calculation time.

(3) The response surface function was employed to establish the explicit optimization model of the fifth-order modal frequency of the door. The modal frequency of the door was optimized, the modal frequency separation between the door and the body in white was realized, and the door was made lighter. The side-impact performance was not reduced significantly.

Data Availability

All data, models, and code generated or used during the study appear in the submitted article.

Conflicts of Interest

The authors declare that they have no conflicts of interest.

Acknowledgments

The authors would like to thank the National Key Research and Development Project of China (no: 2016YFD0700704B) for the support given to this research.

References

[1] J.-K. Shin, K.-H. Lee, S.-I. Song, and G.-J. Park, "Automotive door design with the ULSAB concept using structural optimization," *Structural and Multidisciplinary Optimization*, vol. 23, no. 4, pp. 320–327, 2002.

[2] J. Fang, Y. Gao, G. Sun, and Q. Li, "Multiobjective reliability-based optimization for design of a vehicle door," *Finite Elements in Analysis and Design*, vol. 67, pp. 13–21, 2013.

[3] G. Sun, D. Tan, X. Lv, X. Yan, Q. Li, and X. Huang, "Multi-objective topology optimization of a vehicle door using multiple material tailor-welded blank (TWB) technology," *Advances in Engineering Software*, vol. 124, pp. 1–9, 2018.

[4] K.-H. Lee and D.-H. Kang, "Structural optimization of an automotive door using the kriging interpolation method," *Proceedings of the Institution of Mechanical Engineers, Part D: Journal of Automobile Engineering*, vol. 221, no. 12, pp. 1525–1534, 2007.

[5] P. Zhu, Y.-L. Shi, K.-Z. Zhang, and Z.-Q. Lin, "Optimum design of an automotive inner door panel with a tailor-welded blank structure," *Proceedings of the Institution of Mechanical Engineers, Part D: Journal of Automobile Engineering*, vol. 222, no. 8, pp. 1337–1348, 2008.

[6] X. Cui, S. Wang, and S. J. Hu, "A method for optimal design of automotive body assembly using multi-material construction," *Materials & Design*, vol. 29, no. 2, pp. 381–387, 2008.

[7] E. Talay and A. Altinisik, "The effect of door structural stiffness and flexural components to the interior wind noise at elevated vehicle speeds," *Applied Acoustics*, vol. 148, pp. 86–96, 2019.

[8] A. Ghadianlou and S. B. Abdullah, "Crashworthiness design of vehicle side door beams under low-speed pole side impacts," *Thin-Walled Structures*, vol. 67, pp. 25–33, 2013.

[9] G. E. P. Box and J. S. Hunter, "Multi-factor experimental designs for exploring response surfaces," *The Annals of Mathematical Statistics*, vol. 28, no. 1, pp. 195–241, 1957.

[10] C. Zhang, L. Song, C. Fei, C. Lu, and Y. Xie, "Advanced multiple response surface method of sensitivity analysis for turbine blisk reliability with multi-physics coupling," *Chinese Journal of Aeronautics*, vol. 29, no. 4, pp. 962–971, 2016.

[11] G. Xu, H. Zhang, Q. Zou, and Y. Jin, "Predicting and analyzing interaction of the thermal cloaking performance through response surface method," *International Journal of Heat and Mass Transfer*, vol. 109, pp. 746–754, 2017.

[12] L. Yang, J. Wang, X. Sun, and M. Xu, "Multi-objective optimization design of spiral demister with punched holes by combining response surface method and genetic algorithm," *Powder Technology*, vol. 355, pp. 106–118, 2019.

[13] T. Z. Li and X. L. Yang, "An efficient uniform design for Kriging-based response surface method and its application," *Computers and Geotechnics*, vol. 109, pp. 12–22, 2019.

[14] K.-H. Lee, J.-K. Shin, S.-I. Song, Y.-M. Yoo, and G.-J. Park, "Automotive door design using structural optimization and design of experiments," *Proceedings of the Institution of Mechanical Engineers, Part D: Journal of Automobile Engineering*, vol. 217, no. 10, pp. 855–865, 2003.

[15] R. Ganguli, "Optimum design of a helicopter rotor for low vibration using aeroelastic analysis and response surface methods," *Journal of Sound and Vibration*, vol. 258, no. 2, pp. 327–344, 2002.

[16] H. Sun and S. Lee, "Response surface approach to aerodynamic optimization design of helicopter rotor blade," *International Journal for Numerical Methods in Engineering*, vol. 64, no. 1, pp. 125–142, 2005.

[17] M. De Munck, D. Moens, W. Desmet, and D. Vandepitte, "A response surface based optimisation algorithm for the calculation of fuzzy envelope FRFs of models with uncertain properties," *Computers & Structures*, vol. 86, no. 10, pp. 1080–1092, 2008.

[18] N. S. M. El-Tayeb, T. C. Yap, V. C. Venkatesh, and P. V. Brevern, "Modeling of cryogenic frictional behaviour of titanium alloys using Response Surface Methodology approach," *Materials & Design*, vol. 30, no. 10, pp. 4023–4034, 2009.

[19] Y.-S. Nam, Y.-I. Jeong, B.-C. Shin, and J.-H. Byun, "Enhancing surface layer properties of an aircraft aluminum alloy by shot peening using response surface methodology," *Materials & Design*, vol. 83, pp. 566–576, 2015.

[20] N. Kaya, İ. Karen, and F. Öztürk, "Re-design of a failed clutch fork using topology and shape optimisation by the response surface method," *Materials & Design*, vol. 31, no. 6, pp. 3008–3014, 2010.

[21] Z. Li and X. Liang, "Vibro-acoustic analysis and optimization of damping structure with response surface method," *Materials & Design*, vol. 28, no. 7, pp. 1999–2007, 2007.

[22] T. Goel, R. Vaidyanathan, R. T. Haftka, W. Shyy, N. V. Queipo, and K. Tucker, "Response surface approximation of pareto optimal front in multi-objective optimization," *Computer Methods in Applied Mechanics and Engineering*, vol. 196, no. 4–6, pp. 879–893, 2007.